Optimization of parameters applied to degradation and mineralization of p-nitrophenol using advanced oxidative processes

Vanessa Santolin
UFFS: Universidade Federal da Fronteira Sul
Gabriel André Tochetto (tochettogabriel@gmail.com)
UFFS: Universidade Federal da Fronteira Sul https://orcid.org/0000-0003-1656-505X
Adriana Dervanoski
UFFS: Universidade Federal da Fronteira Sul
Gean Delise Leal Pasquali
UFFS: Universidade Federal da Fronteira Sul

Research Article

Keywords: Photocatalysis, Photolysis, Photo-peroxidation, Phenolic compounds

Posted Date: July 9th, 2021

DOI: https://doi.org/10.21203/rs.3.rs-700299/v1

Optimization of parameters applied to degradation and mineralization of p-nitrophenol using advanced oxidative processes

Vanessa Santolin[1], Gabriel André Tochetto[1,2], Adriana Dervanoski[1], Gean Delise Leal Pasquali[1,3]*

[1]Laboratory of Effluent and Waste (LAER), Department of Environmental and Sanitary Engineering (EAS), Federal University of Fronteira Sul (UFFS), 997000-970, Erechim, Rio Grande do Sul, Brazil

[2]Laboratory of Numerical Simulation of Chemical Systems and Mass Transfer (LabSIN-LabMASSA), Department of Chemical and Food Engineering (EQA), Federal University of Santa Catarina (UFSC), 88040-900, Florianópolis, Santa Catarina, Brazil

[3]Post-Graduation Program in Science and Environmental Technology (PPGCTA), Federal University of Fronteira Sul (UFFS), 997000-970, Erechim, Rio Grande do Sul, Brazil

* Corresponding author: Gabriel André Tochetto, e-mail: tochettogabriel@gmail.com, phone: + 55 (54) 99664-0195

E-mail addresses: Vanessa Santolin (vane.santolin22@gmail.com), Gabriel André Tochetto (tochettogabriel@gmail.com), Adriana Dervanoski (adriana.dervanoski@uffs.edu.br), Gean Delise Leal Pasquali (geandelise@uffs.edu.br)

Abstract

Advanced oxidative processes are widely used in the degradation of organic compounds. The degradation and mineralization of the PNF was evaluated by means of an experimental factorial design, using photolysis (UV) and photo-peroxidation (UV/H_2O_2). With the results optimized, degradation kinetics was performed and the experimental data adjusted to mathematical models. In the UV system, it was possible to degrade just over 65% and mineralize 15% over 7 h of reaction; however, with the addition of the oxidizing agent H_2O_2, it was possible to obtain 100% removal of the contaminant, suggesting that there was no formation of intermediate compounds. Kinetics results fitting the first order model and the velocity constants revealed that degradation is extremely faster in the UV/H_2O_2 system ($k_{1,UV/H2O2} = 0.0580\ min^{-1} > k_{1,UV} = 0.0018\ min^{-1}$).

Keywords: Photocatalysis; Photolysis; Photo-peroxidation; Phenolic compounds.

1. Introduction

Degradation of the quality of aquatic systems due to the disposal of toxic liquid waste is a significant issue today (Khairy et al. 2020). Organic pollutants in the class of phenolic compounds are found in wastewater because of their extensive use in industry (Liu et al. 2020; Wang et al. 2020). Even in low concentrations, these pollutants present a great risks to health (Xiong et al. 2019; Liang et al. 2020) and ecosystems (Li et al. 2020). Nitrophenols (NFs) are composed of benzene rings with bonds of nitro (-NO) and hydroxyl (-OH) groups, are widely used in the synthesis of dyes, paints, pesticides, herbicides, solvents, in the plastic, leather and pharmaceutical industry (Zhang et al. 2017; Chen et al. 2017; Xiong et al. 2019). NFs and their derivates have high toxicity, carcinogenicity and bioaccumulation (Ibrahim et al. 2019; Wang et al. 2021a), with *p*-nitrophenol (PNF) being listed as a priority pollutant by the United States Environmental Protection Agency (USEPA) (Tugba Saka and Tekintas 2020). In Brazil, the maximum level of phenols allowed is only 0.5 mg L^{-1} (Brasil 2011). Therefore, it becomes necessary to develop effective methods to degrade NFs and their derivates.

Conventional treatments used in industries aren't completely effective in removing NFs (Hu et al. 2020). These technologies are unable to degrade or mineralize complex organic components (Mukherjee et al. 2020) with high mobility and low biodegradability in high concentrations (Hu et al. 2020). In addition, phenol removal processes, which involve sorption and biodegradation, are slow and, in some cases, inefficient (Ren et al. 2017; Zhang et al. 2017; Jiang et al. 2018). Advanced oxidation processes (AOPs) are widely used and promising technologies, as they provide highly active oxidants to remove persistent organic pollutants (Mukherjee et al. 2020), such as NFs in aqueous solution (Dewil et al. 2017; Abazari et al. 2019; Wang et al. 2021b). Photocatalytic oxidation is seen as an effective, viable and low-cost treatment to remove pollutants from aqueous solutions (Xiong et al. 2019). Hazardous pollutants can be mineralized under environmental conditions using this technique (García and Hodaifa 2017; Rodrigues et al. 2018; Athanasekou et al. 2018; Fernandes et al. 2019). In the photo-peroxidation process (UV/H_2O_2), two hydroxyl radicals (*OH) are formed when the hydrogen peroxide is exposed to UV light (200-280 nm), by breaking the O_2 bond (Ledakowicz et al. 2019). UV/H_2O_2 has advantages over conventional and biological chemical treatments, mainly due to the easy availability of commercial peroxide, the thermal stability, and the non-formation of sludge (Yassumoto et al. 2009).

The purpose of this study was to evaluate the influence of the main parameters used in the UV and UV/H_2O_2 systems through an experimental planning design to optimize the degradation and mineralization of PNF, while evaluating the kinetics parameters of degradation of the two AOPs.

2. Material and methods

2.1 Batch photochemical reactor

The experimental design tests and kinetics degradation were performed in a rectangular reactor, with dimensions 15 x 45 cm. The reactor was equipped with a UV lamp (36 W, λ = 254 nm) as a radiation source, positioned in the center of the reactor, 10 cm from the surface of the liquid (Fig. 1). The operation was carried out under ambient conditions of temperature (25 ± 3°C) and pressure, constant agitation of 150 rpm, and isolated in order to avoid dissipation and irradiation to the external environment.

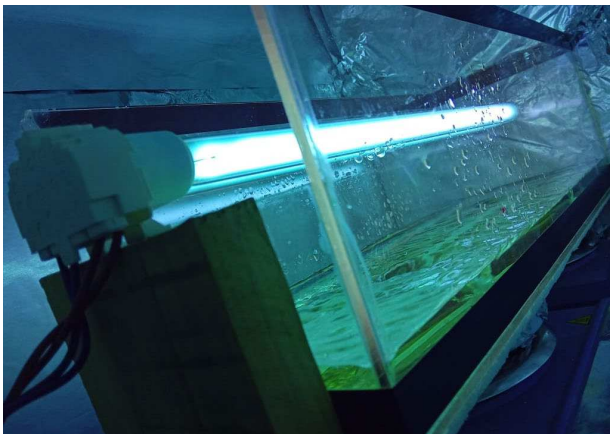

Fig. 1 Photochemical reactor containing UV lamp and PNF solution during the advanced oxidative process.

2.2 Experimental design and procedure

The experiments were designed with a central composite design (CCD) 2^2 with 8 tries and 3 repetitions at the central point (Table 1). In the UV-only experiments, the PNF concentration (10-100 mg L^{-1}) and height of the water depth (1.5-3.5) were the variables evaluated, while in UV/H_2O_2, the PNF (10-150 mg L^{-1}) and H_2O_2 (10-100 mg L^{-1}) concentrations were evaluated. For photo-peroxidation, the liquid blade was fixed at 2.5 cm (best UV result). The PNF ($C_6H_5NO_3$) (99%, Sigma-Aldrich) and hydrogen peroxide (H_2O_2) (30%, Êxodo Científica) solutions used were prepared in deionized water.

Table 1 CCD experimental planning matrix for direct photolysis and UV/H_2O_2 with coded and actual values.

Assay	UV		UV/H_2O_2	
	PNF (mg L^{-1})	Water depht (cm)	PNF (mg L^{-1})	H_2O_2 (mg L^{-1})
1	(-1) 15	(-1) 2	(-1) 15	(-1) 30
2	(-1) 15	(+1) 3	(+1) 50	(-1) 30

3	(+1) 50	(-1) 2	(-1) 15	(+1) 100
4	(+1) 50	(+1) 3	(+1) 50	(+1) 100
5	(0) 30	(-1.41) 1.5	(-1.41) 10	(0) 50
6	(-1.41) 10	(0) 2.5	(0) 30	(-1.41) 10
7	(0) 30	(+1.41) 3.5	(+1.41) 100	(0) 50
8	(+ 1.41) 100	(0) 2.5	(0) 30	(+1.41) 150
9	(0) 30	(0) 2.5	(0) 30	(0) 50
10	(0) 30	(0) 2.5	(0) 30	(0) 50
11	(0) 30	(0) 2.5	(0) 30	(0) 50

The aqueous PNF solution was added to the reactor together with H_2O_2 (only for UV/H_2O_2). The system was operating for 420 min for UV and 150 min for UV/H_2O_2. The pH, PNF concentration and TOC were determined at the beginning and end of the process. The residual H_2O_2 concentration was also analyzed in the photo-peroxidation system.

2.3 Analytical methods

pH assessment was performed with a digital pHmeter (Tecnopon, mPA210), using the potentiometric method (APHA et al. 1999). The PNF concentration of the samples was evaluated by the direct photometric method (Al-Asheh et al. 2004) on a spectrophotometer (Nova Instruments, NI 1600UV) at a wavelength λ = 400 nm. For evaluation of total organic carbon (TOC) removal, an automatic analyzer was used (Shimadzu, TOC-5000) (APHA et al. 1999). The residual H_2O_2 after reaction was determined by the colorimetric method with MQuant® (Merck) (0 - 100 mg L^{-1} H_2O_2).

The experimental data was treated using the Statistica 12.0 (StatSoft, Tulsa, USA) and the results were validated with analysis of variance (ANOVA). The response surface methodology (SRM) obtained an optimization of the advanced oxidation processes, with 95% confidence (p-value < 0.05).

The degradation of PNF in photolysis and UV/H_2O_2 were evaluated by their fitness to the non-linear mathematical models of first order (FO), pseudo-first order (PSO) and second order (SO) (Eq. 1-3, respectively), using Statistica 12.0 (StatSoft, Tulsa, USA), with 95% confidence (p-value < 0.05).

$$C = C_i e^{-k_1 t} \quad (1)$$

$$C = C_e + (C_i - C_e) e^{-k_{p1} t} \quad (2)$$

$$C = C_i \frac{1}{1 + k_2 C_i t} \quad (3)$$

where *Ci* and *Ce* are the initial and equilibrium concentration of PNF (mg L^{-1}), *t* is the reaction time (min). The velocity constants k_1 (min^{-1}), k_{p1} (min^{-1}) e k_2 (L mg^{-1} min^{-1}) refer to the FO, PFO and SO models.

3. Results and discussion

3.1 Optimization of PNF degradation

The degradation of PNF in the UV and UV/H_2O_2 systems is show in Fig. 2. It is possible to observe that the best percentage results of PNF degradation occurred in the presence of the oxidizing agent H_2O_2. For the UV system, the best result occurred in low concentrations of the contaminant (15 mg L^{-1}) and liquid slide of 2 cm, reaching a degradation of about 65% of the PNF. However, it took 7 hours of operation to achieve this result, which makes it unfeasible due to the residence time of the batch treatment, as well as the energy consumption, resulting in an increase in the system's operating cost. The treatment using only UV irradiation is not effective in the treatment of waste water containing organic compounds, as was also observed in the work of Datta et al. (2004), since it is a lengthy process and degrades the contaminant at significantly lower rates (Zhao et al. 2010). In the present study, for a concentration of 10 mg L-1, it took 7 hours of experiment to obtain a degradation of about 63%. This result is similar to that found by Zhao et al. (2010), who needed 12 hours to degrade 75% of the initial concentration (10 mg L-1).

For the UV/H_2O_2 process, the degradation of the contaminant (Fig. 2) reached a value close to 100% in several tests, presenting values below 85% only in the axial points, where the combination of the conditions is more extreme (lower H_2O_2 concentration and higher PNF concentration). Ibrahim et al. (2019) studied a photocatalytic process in the presence of a titanium dioxide (TiO_2) ferrite nanotube to treat 10 mg L-1 of PNF, obtaining 100% photocatalytic reduction of contaminant in a maximum time of 55 minutes. Thinh et al. (2020), after 50 minutes of photocatalytic treatment, reached a maximum yield of 94% when treating 20 mg L-1 of PNF. These results demonstrate the importance of hydrogen peroxide as an effective, viable and ecologically efficient method to increase the hydroxyl radicals and the reaction yield, decreasing the reaction time and cost of the process. In this study, it was possible to degrade 100% of the contaminant using higher concentrations of PNF, with similar concentrated ratios of H_2O_2, in better reaction time conditions, of 10, 30, 70 and 120 minutes. Datta et al. (2004) used a UV/H_2O_2 system to degrade 15 mg L^{-1} of PNF, degrading 100% of the contaminant in 5 hours of testing, using a 8 W mercury lamp. The experimental tests carried out in this work demonstrated the capacity for degradation under pollutant and hydrogen peroxide concentrations at much lower ratios, which makes these results interesting from an economic point of view, given the lower energy and input consumption.

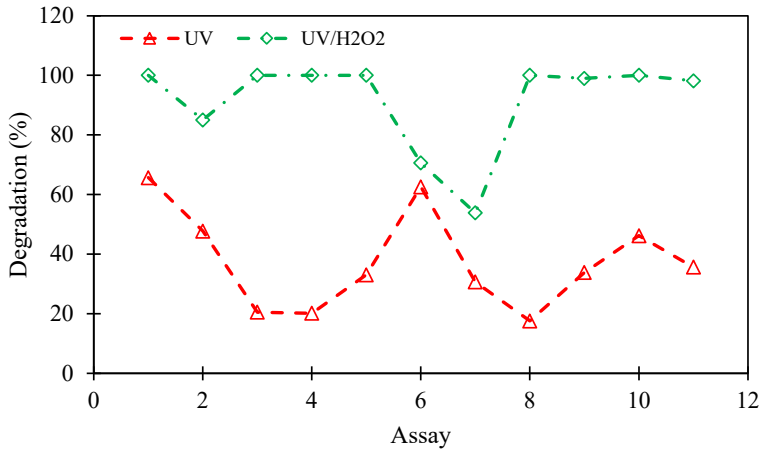

Fig. 2 Percentages of PNF degradation obtained from the experimental design for the UV and UV/H_2O_2 system.

In the Pareto diagram (Fig. 3), it is possible to visualize the influence of the studied variables in the applied treatments. As a planning response, for the degradation in the UV-only system (Fig. 3a), the linear and quadratic

term of the contaminant concentration were statistically significant in the oxidation reaction of the PNF. As the linear term had a negative effect (-7.84156), it can also be concluded that the greatest efficiency of degradation occurs in lower concentrations of PNF. For the effects of contaminant degradation by the UV/H_2O_2 process (Fig. 3b), it is possible to observe the direct influence of the primary oxidizing agent H_2O_2 in the linear and quadratic term. The linear term (+4.10551) indicates that PNF degradation is enhanced in higher concentrations of peroxide. This effect was also observed by Wang et al. (2021b) when treating 10 mg L^{-1} of PNF through the photo-fenton process in continuous flow for approximately 4 hours, in which he observed that the reaction rate increases as H_2O_2 is added in the system. The author increased the efficiency from 35% to 84% of PNF degradation by increasing the peroxide concentration from 68 mg L^{-1} to 170 mg L^{-1}. The increase in catalysis performance by increasing H_2O_2 concentrations was also observed by Khairy et al. (2020).

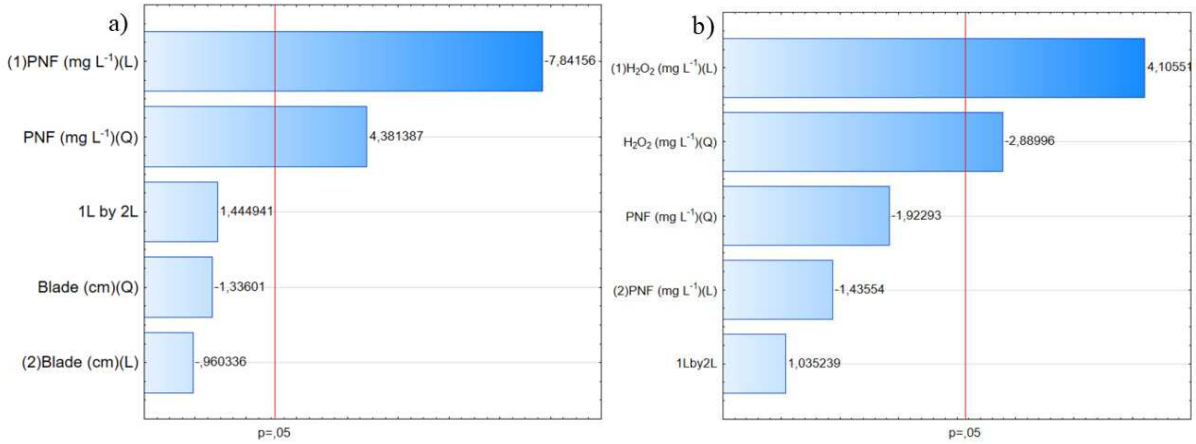

Fig. 3 Pareto chart of effects for PNF degradation in the UV (a) and UV/H_2O_2 (b) system.

From the calculation of the effects of the studied factors, as well as the possible interactions, an optimized parameterized model was obtained to describe the PNF degradation for the UV-only (Eq. 4) and UV/H_2O_2 (Eq. 5) processes. The percentage of explained variation (R^2) obtained by the models was 94.33% for the UV-only process and 92.55% for the UV/H_2O_2 system, showing good adjustment to the experimental data.

$$UV\ Degradation\ (mg\ L^{-1}) = 84.155 - 2.840x + 0.010x^2 + 14.663y - 6.487y^2 + 0.451xy \quad (4)$$

$$UV/H_2O_2\ Degradation\ (mg\ L^{-1}) = 82.588 - 0.528x + 0.003x^2 + 0.174y - 0.005y^2 + 0.004xy \quad (5)$$

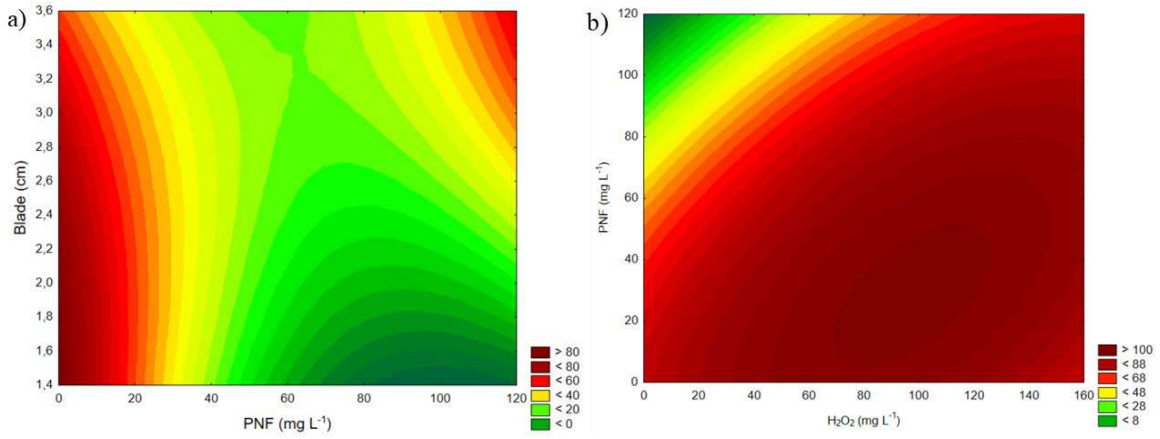

Fig. 4 Response surface for PNF degradation in the UV-only (a) and UV/H_2O_2 (b) system.

Optimized conditions of PNF concentration, water depth and H_2O_2 concentration are obtained (Fig. 4) from the contour surfaces generated by the model. It is possible to verify, from the contour curve (Fig. 4a), that the optimal degradation conditions in the presence of UV light only occurs for concentrations of up to 10 mg L^{-1} of contaminant ($C_6H_5NO_3$) and at a water depth of effluent to be treated between 1.4 cm and 2.5 cm, obtaining in these conditions up to 80% of degradation in the maximization of the process. ANOVA (Table SM1) confirms that these results are statistically significant (Fcalc> Ftab) and reliably represent the results (Fig. SM1).

The optimal range for degradation in the UV/H_2O_2 process (Fig. 4b) indicates that the PNF concentration, under the conditions evaluated, can reach up to 60 mg L^{-1}, and the H_2O_2 concentration between 50 and 130 mg L^{-1}. In addition to increasing the degradation efficiency at concentrations above 50 mg L^{-1} of H_2O_2, the experimental tests showed that the increase in the initial concentration of peroxide contributed to the decrease in reaction time, since the primary oxidant is responsible for the formation of hydroxyl radicals. When the ratio between the concentrations of the oxidizing agent and the contaminant was 5:1 and 6:1, the kinetics were favored; that is, when the H_2O_2 concentration was 5 and 6 times the stoichiometric dose of $C_6H_5NO_3$, the kinetics obtained the equilibrium of reaction faster, in less than 20 minutes, and managed to degrade 100% of PNF. The same did not occur in the tests where the peroxide content corresponded to 2 and 1.7, 0.6, and 0.5 of H_2O_2 of the stoichiometric dose of the PNF. In these tests, the reaction times were longer, varying between 70 and 150 minutes, and degradations of 85%, 70% and 53% were obtained in the longest reaction time. Using ANOVA (Table SM2), it is possible to confirm that these results are statistically significant (F_{calc}> F_{tab}) and reliably represent the results (Fig. SM1).

3.2 Optimization of PNF mineralization

The contaminant mineralization was evaluated by removing TOC, that is, the amount of total organic concentration oxidized to CO_2 and H_2O, which was an important indicator of process effectiveness. Regarding mineralization in the direct photolysis process (Fig. 5), no significant values of TOC removal were found, reaching a maximum of 15.76% for the lowest concentrations of the contaminant (15 mg L^{-1}) associated with lower water depth (2 cm).

The removal of TOC for the UV/H_2O_2 assays (Fig. 5) obtained better results compared to the treatment using only UV radiation. About 100% of the PNF was mineralized in the test conducted with the lowest concentration of pollutant studied (10 mg L^{-1}) in the presence of 50 mg L^{-1} of H_2O_2. In the other tests, some TOC level persisted, depending on the concentration of the contaminant; that is, with the increase in PNF concentration, the concentration of carbon present in the sample after treatment is higher, with lower removal rates being observed. Ledakowicz et al. (2019) states that the persistence of high carbon concentration is characteristic of UV/H_2O_2, compared to other advanced oxidative processes.

The permanence of some TOC, even in the tests that obtained degradation of 100% of p-nitrophenol, indicates the formation of intermediate compounds that are resistant to degradation by the UV/H_2O_2 process. That is because, as Xiong et al. (2019) points out, compounds with lower toxicity may be formed (Wang et al. 2021a). P-nitrophenol may have been broken down into low-toxicity p-aminophenol, as well as its byproducts: benzoquinone, hydroquinone and molecular carboxylic acids (Li et al. 2017). Xiong et al. (2018) states that the PNF can be directly oxidized to hydroquinone and benzoquinone, and later to carboxylic acids. When PNF in an aqueous solution is subjected to an advanced oxidation process, intermediate compounds occur in the solution, such as phenol, catechol and p-nitrocatechol, 2,4-DNP, p-benzoquinone, oxalic acid, and acetic acid (Rodrigues et al. 2018; Wang et al. 2021a).

The acidic compounds formed during the oxidative process explain the acidity of the solution after treatment. Before the treatment, the initial pH of the solution coincided with the natural pH of the PNF in aqueous solution, being in the range of 5.5 to 6.6 (Li et al. 2019). At the end of the reaction time, the measured pH remained in the range of 3.2 and 4.1, in all tests. The reduction in pH is associated with the production of anions of organic and inorganic acids during the photochemical process, as mentioned by Shu and Chang (2005). The formation of intermediate compounds increases as the initial concentration of PNF is increased, and because these intermediates are highly reactive to hydroxyl radicals, they can reduce the removal efficiency (Daneshvar et al. 2007). The final pH of the treatments using only UV radiation remained slightly acidic, between 5.2 and 6.1. The behavior of the pH close to the natural PNF pH and the low TOC removal shows that, in the direct photolysis system, even in tests that reached values above 60% of degradation, the presence of the contaminant persists at the end of the treatment, as well as that of possible intermediate compounds resulting from the molecular changes undergone by it during photolysis.

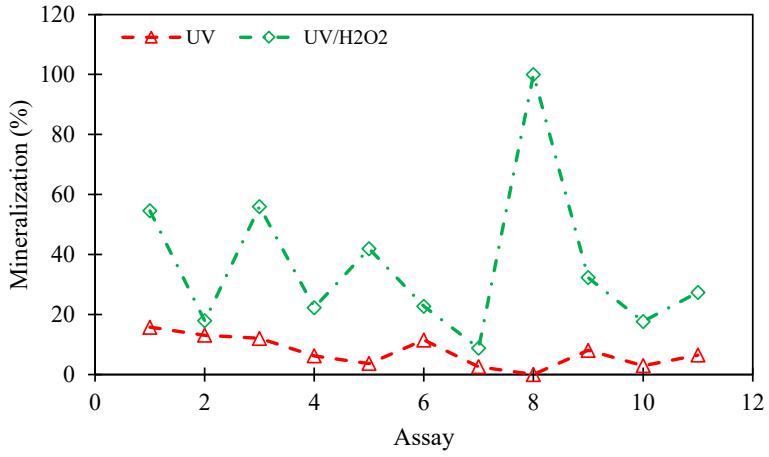

Fig. 5 Percentages of PNF mineralization obtained from the experimental design for the UV-only and UV/H_2O_2 system.

In the Pareto diagram (Fig. 6), it can be seen that, in the mineralization process using the UV-only system (Fig. 6a), there was no significance for the studied variables, PNF concentration and water depth, within the conditions evaluated. For the UV/H_2O_2 tests (Fig. 6b), however, the diagram points to the direct influence of the linear term of PNF concentration (-3.80903) and the quadratic term referring to hydrogen peroxide for mineralization, with the negative value of variable PNF (linear) suggesting that, at lower concentrations of the contaminant, the mineralization would be higher.

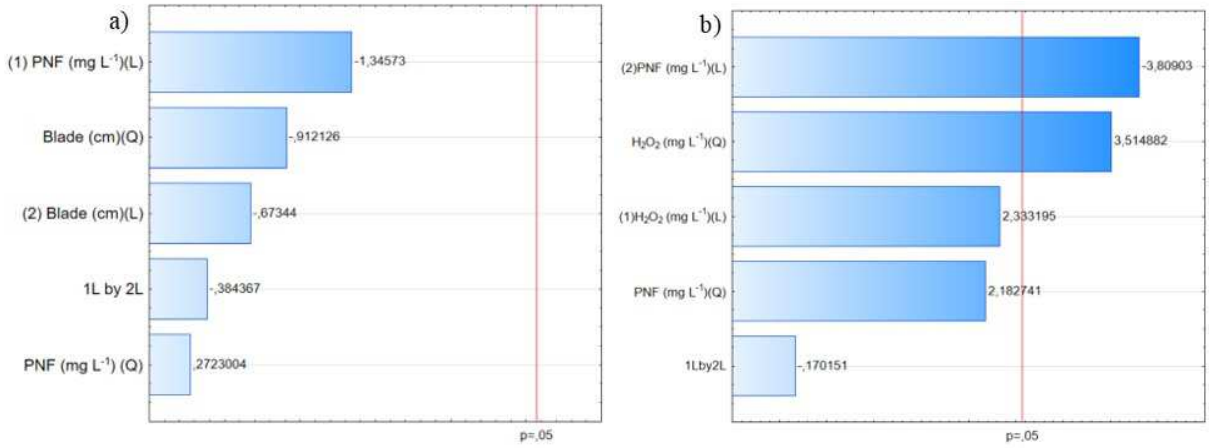

Fig. 6 Pareto chart of effects for PNF mineralization in the UV-only (a) and UV/H_2O_2 (b) system.

In ANOVA (Table SM3), it appears that, in the UV-only system, the mineralization was not significant ($F_{calc} < F_{tab}$) and did not present a good correlation of the data (Fig. SM3), thus it was not possible to obtain an equation capable of predicting the removal of TOC. However, in the UV/H_2O2 system, ANOVA (Table SM4) confirms the reliability of the results (Fig. SM4), making it possible to obtain a parameterized model (Eq 6) that manages to represent about 92.44% of the data.

$$UV/H_2O_2\ Mineralization\ (mg\ L^{-1}) = 75.552 - 0.630x + 0.006x^2 - 1.481y + 0.010y^2 - 0.001xy \quad (6)$$

Fig. 7 shows the contour curves for TOC mineralization in UV/H_2O_2 tests. The maximum removal of PNF occurred in low concentrations of contaminant (< 10 mg L^{-1}) and H_2O_2 concentrations above 150 mg L^{-1}.

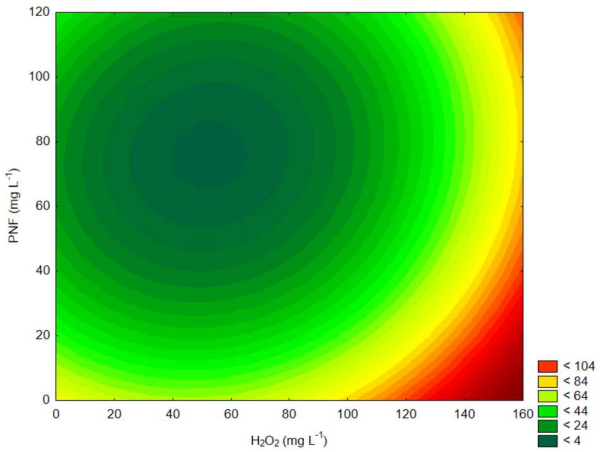

Fig. 7 Response surface for PNF mineralization in the UV/H_2O_2 system.

In a photocatalytic process with the presence of H_2O_2, it is important to optimize the dose of the oxidizer, since the excess increases the cost of the process and can eliminate the hydroxyl radicals formed (Rodrigues et al. 2018). Thus, the residual peroxide concentration was evaluated at the end of the degradation time in the experimental tests. The higher the concentration of the contaminant, the greater the consumption of H_2O_2 in the system. For example, in PNF concentrations higher than 30 mg L^{-1}, consumption of the oxidant was greater than 60% in all tests, reaching 80%. The tests with a contaminant concentration of 50 and 100 mg L^{-1} obtained consumption of 70% H_2O_2, consequently, a residual content of 30%. The residual content of the oxidizing agent quantified at the end of the treatment does not interfere in the oxidative capacity, since, in tests 3 and 8, there was a residual content of 90 and 140 mg L^{-1}, respectively, and these conditions allowed for 100% degradation of the nitrophenolic compound. Thus, excess peroxide present in the experimental tests of this study did not lead to the elimination of hydroxyl radicals. Rodrigues et al. (2018) points out the disadvantage of overdosing the oxidative agent. The disadvantage of overdosing applies to the oxidant waste, since there was an excellent degradation of 50 and 30 mg L^{-1} of the contaminant with less residual content, 30 and 20 mg L^{-1}, respectively, in test 4 and in the central point triplicate (tests 9, 10 and 11).

3.3 Modeling kinetics

Fig. 8 shows the experimental results of the kinetic tests and the adjustment through the models, where the best performance was obtained for each of the studied systems. For the UV-only system, an initial concentration of 15 mg L^{-1} was used, while for the UV/H_2O_2 system the concentration was 30 mg L^{-1}. In the UV-only system (Fig. 8a), it is noticed that the degradation of the contaminant does occur; however, very long times (400 min) are required, making the process unfeasible. For the UV/H_2O_2 system, the degradation of the PNF was effective and faster (70 min) when compared to the system with the presence of UV light only.

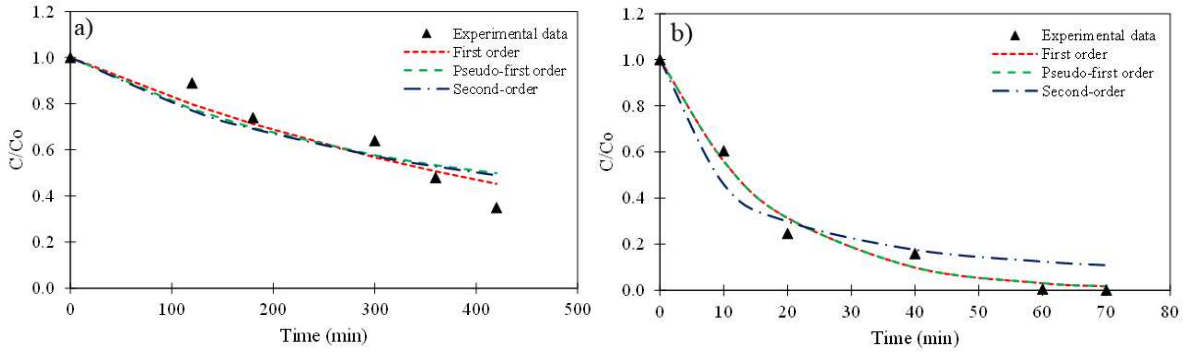

Fig. 8 Experimental results and fitness to mathematical models of first order (FO), pseudo-first order (PFO) and second order (SO) for PNF degradation of the UV-only and UV/H_2O_2 systems.

The experimental results for PNF degradation obtained in the treatments with UV-only and UV/H_2O_2 were adjusted to the first order, pseudo-first order and second order models. In Fig. 8, it is possible to observe that the mathematical models evaluated showed good adjustments to the experimental data. In Table 3, it was found that the determination coefficient (R^2) for the UV system, a first-order model, represented the experimental data with greater precision, obtaining a k_1 constant of 0.0018 min^{-1} with 99% reliability (p-value <0.001). For the UV/H_2O_2 system, two models were able to reproduce the experimental results (first order and pseudo-first order), also with reliability greater than 99% (p-value <0.001) and good R^2 (0.9927), where the speed constants k_1 and k_{p1} found were 0.0580 min^{-1}.

The rate of degradation for the UV/H_2O_2 system was higher when compared to the UV system (0.0580 min^{-1}> 0.0018 min^{-1}), where this result is expected, since the presence of H_2O_2 potentiates the oxidation reaction, due to greater amount of *OH produced. According to the study by Zhao et al. (2012), the velocity constant is affected by the pH of the solution, and the rate of degradation in acidic pH is higher when compared to values closer to neutrality and alkalis. In this study, it was observed that the pH at the end of the oxidation process in the presence of only UV light varied between 5.2 to 6.1, while in the UV/H_2O_2 system the pH showed more acidic characteristics, oscillating between 3.2 and 4.1. It should be noted that the initial PNF concentration has a direct influence on the degradation rate constant (Zhao et al. 2012).

Table 3 Results of the kinetics constants of PNF degradation in the UV/H_2O_2 system.

Mathematical model	UV	UV/H_2O_2
First order		
k_1 (min^{-1})	0.0018 ± 0.0002	0.0580 ± 0.0049
p-value	0.0002	< 0.0001
R^2	0.9559	0.9927
Pseudo-first order		
k_{p1} (min^{-1})	0.0035 ± 0.0006	0.0580 ± 0.0049
p-value	0.0033	< 0.0001
R^2	0.9241	0.9927
Second order		
k_2 (L mg^{-1} min^{-1})	0.0001 ± 0.0001	0.0039 ± 0.0010
p-value	0.0027	0.0010
R^2	0.9257	0.9672

The PNF degradation rates found are consistent with the results observed in the literature. The work of Zhao et al. (2012) investigated the removal of the same contaminant (C_o = 100 mg L^{-1}) under different AOPs, obtaining a constant k_{p1} of 0.012 min^{-1} for degradation in the presence of ultrasound (US) irradiation, 0.035 min^{-1} using Fenton and 0.097 min^{-1} in the combination of these processes (US/Fenton). The combination of AOPs is a strategy to increase the efficacy of the treatment. In the kinetic study of Li et al. (2020), it was found that the pseudo-first order model also obtained the best fit; however, the velocity constant k_{p1} (0.0002 min^{-1}) for the combined UV/H_2O_2 system was much lower than that observed both in the UV-only system and the UV/H_2O_2 combination found in this work. Another possibility to improve the efficiency of AOP is the use of catalysts that aim to increase the reaction speed. The constant k_1 obtained in the work of Li et al. (2020) for the combination of the UV/H_2O_2 system with iron-based catalysts reached 0.0415 min^{-1} (UV/Fe-PAN/H_2O_2) and 0.2247 min^{-1} (UV/Fe-HPAN/H_2O_2).

4. Conclusion

In the present study, AOPs were used to evaluate the degradation and mineralization of the PNF present in aqueous solutions, using a photochemical batch reactor. The UV-only system was not effective due to the high residence time and the low removal of NFs. However, the use of H_2O_2 in low concentrations combined with ultraviolet radiation has shown to be promising for the treatment of wastewater containing PNF in low concentrations, as it obtained the complete removal of PNF. The first-order kinetics model of degradation represented the results. The k_1 constants prove that combining the processes increases the rate of degradation ($k_{1,UV/H2O2}$ = 0.0580 min^{-1} > $k_{1,UV}$ = 0.0018 min^{-1}). The intermediate compounds formed in the degradation process are of reduced toxicity compared to the priority compound studied in this work.

Declarations

Ethics approval and consent to participate

Not applicable.

Consent for publication

Not applicable.

Availability of data and materials

Not applicable.

Competing interests

The authors declare that they have no competing interests. All authors certify that they have no affiliations with or involvement in any organization or entity with any financial interest or non-financial interest in the subject matter or materials discussed in this manuscript.

Funding

Not applicable.

Author's contributions

All authors contributed to the study conception and design. Material preparation and data collection were performed by Vanessa Santolin and Gabriel André Tochetto. Analysis data were performed by Gabriel André Tochetto, Adriana Dervanoski and Gean Delise Leal Pasquali. The first draft of the manuscript was written by Vanessa Santolin and Gabriel André Tochetto. All authors commented on previous versions of the manuscript. All authors read and approved the final manuscript.

Acknowledgments

The authors are pleased to acknowledge: to Federal University of Fronteira Sul (UFFS), to the Analytical Center of the Erechim *campus*, to the Fincancer of Studies and Projetcs (FINEP) and to the Laboratory Technicians, especially Suzana and Denys for the analyzes performed.

References

Abazari R, Mahjoub AR, Salehi G (2019) Preparation of amine functionalized g-C3N4@H/SMOF NCs with visible light photocatalytic characteristic for 4-nitrophenol degradation from aqueous solution. J Hazard Mater 365:921–931. https://doi.org/10.1016/j.jhazmat.2018.11.087

Al-Asheh S, Banat F, Masad A (2004) Kinetics and equilibrium sorption studies of 4-nitrophenol on pyrolyzed and activated oil shale residue. Environ Geol 45:1109–1117. https://doi.org/10.1007/s00254-004-0969-4

APHA APHA, AWWA AWWA, WEF WEF (1999) Standard Methods for the Examination of Water and Wastewater. In: Standard Methods for the Examination of Water and Wastewater. p 733

Athanasekou CP, Likodimos V, Falaras P (2018) Recent developments of TiO_2 photocatalysis involving advanced oxidation and reduction reactions in water. J Environ Chem Eng 6:7386–7394. https://doi.org/10.1016/j.jece.2018.07.026

Brasil (2011) Resolução n°430 de 13 de maio de 2011. Brasília: Ministério do Meio Ambiente. Conselho Nacional do Meio Ambiente, 2011.

Chen J, Sun X, Lin L, et al (2017) Adsorption removal of o-nitrophenol and p-nitrophenol from wastewater by metal–organic framework Cr-BDC. Chinese J Chem Eng 25:775–781. https://doi.org/10.1016/j.cjche.2016.10.014

Daneshvar N, Behnajady MA, Zorriyeh Asghar Y (2007) Photooxidative degradation of 4-nitrophenol (4-NP) in UV/H_2O_2 process: Influence of operational parameters and reaction mechanism. J Hazard Mater 139:275–279. https://doi.org/10.1016/j.jhazmat.2006.06.045

Datta C, Naidu R, Yenkie MKN (2004) Photo-oxidative degradation of synthetic organic pollutant p-nitrophenol. J Sci Ind Res (India) 63:518–521

Dewil R, Mantzavinos D, Poulios I, Rodrigo MA (2017) New perspectives for Advanced Oxidation Processes. J Environ Manage 195:93–99. https://doi.org/10.1016/j.jenvman.2017.04.010

Fernandes A, Gągol M, Makoś P, et al (2019) Integrated photocatalytic advanced oxidation system (TiO_2/UV/O_3/H_2O_2) for degradation of volatile organic compounds. Sep Purif Technol 224:1–14. https://doi.org/10.1016/j.seppur.2019.05.012

García CA, Hodaifa G (2017) Real olive oil mill wastewater treatment by photo-Fenton system using artificial ultraviolet light lamps. J Clean Prod 162:743–753. https://doi.org/10.1016/j.jclepro.2017.06.088

Hu L, Wang P, Liu G, et al (2020) Catalytic degradation of p-nitrophenol by magnetically recoverable Fe_3O_4 as a persulfate activator under microwave irradiation. Chemosphere 240:124977. https://doi.org/10.1016/j.chemosphere.2019.124977

Ibrahim I, Athanasekou C, Manolis G, et al (2019) Photocatalysis as an advanced reduction process (ARP): The reduction of 4-nitrophenol using titania nanotubes-ferrite nanocomposites. J Hazard Mater 372:37–44. https://doi.org/10.1016/j.jhazmat.2018.12.090

Jiang W, Yang J, Wang X, et al (2018) Phenol degradation catalyzed by a peroxidase mimic constructed through the grafting of heme onto metal-organic frameworks. Bioresour Technol 247:1246–1248. https://doi.org/10.1016/j.biortech.2017.09.161

Khairy M, Naguib EM, Mohamed MM (2020) Enhancement of Photocatalytic and Sonophotocatalytic Degradation of 4-nitrophenol by ZnO/Graphene Oxide and ZnO/Carbon Nanotube Nanocomposites. J Photochem Photobiol A Chem 396:112507. https://doi.org/10.1016/j.jphotochem.2020.112507

Ledakowicz S, Stolarek P, Malinowski A, Lepez O (2019) Thermochemical treatment of sewage sludge by integration of drying and pyrolysis/autogasification. Renew Sustain Energy Rev 104:319–327. https://doi.org/10.1016/j.rser.2019.01.018

Li J, Liu Q, Ji Q qing, Lai B (2017) Degradation of p-nitrophenol (PNP) in aqueous solution by Fe0-PM-PS system through response surface methodology (RSM). Appl Catal B Environ 200:633–646. https://doi.org/10.1016/j.apcatb.2016.07.026

Li X, Li C, Gao G, et al (2020) In-situ self-assembly of robust Fe (III)-carboxyl functionalized polyacrylonitrile polymeric bead catalyst for efficient photo-Fenton oxidation of p-nitrophenol. Sci Total Environ 702:134910. https://doi.org/10.1016/j.scitotenv.2019.134910

Li Z, Sellaoui L, Luiz Dotto G, et al (2019) Understanding the adsorption mechanism of phenol and 2-nitrophenol on a biopolymer-based biochar in single and binary systems via advanced modeling analysis. Chem Eng J 371:1–6. https://doi.org/10.1016/j.cej.2019.04.035

Liang Y, Wang X, Dong S, et al (2020) Size distributions of nitrated phenols in winter at a coastal site in north China and the impacts from primary sources and secondary formation. Chemosphere 250:126256. https://doi.org/10.1016/j.chemosphere.2020.126256

Liu S, Huang B, Zheng G, et al (2020) Nanocapsulation of horseradish peroxidase (HRP) enhances enzymatic performance in removing phenolic compounds. Int J Biol Macromol 150:814–822. https://doi.org/10.1016/j.ijbiomac.2020.02.043

Mukherjee A, Mullick A, Teja R, et al (2020) Performance and energetic analysis of hydrodynamic cavitation and potential integration with existing advanced oxidation processes: A case study for real life greywater treatment. Ultrason Sonochem 66:105116. https://doi.org/10.1016/j.ultsonch.2020.105116

Ren LF, Chen R, Zhang X, et al (2017) Phenol biodegradation and microbial community dynamics in extractive membrane bioreactor (EMBR) for phenol-laden saline wastewater. Bioresour Technol 244:1121–1128. https://doi.org/10.1016/j.biortech.2017.08.121

Rodrigues CSD, Borges RAC, Lima VN, Madeira LM (2018) p-Nitrophenol degradation by Fenton's oxidation in a bubble column reactor. J Environ Manage 206:774–785.

https://doi.org/10.1016/j.jenvman.2017.11.032

Shu HY, Chang MC (2005) Decolorization and mineralization of a phthalocyanine dye C.I. Direct Blue 199 using UV/H_2O_2 process. J Hazard Mater 125:96–101. https://doi.org/10.1016/j.jhazmat.2005.05.016

Thinh DB, Tien NT, Dat NM, et al (2020) Improved photodegradation of p-nitrophenol from water media using ternary $MgFe_2O_4$-doped TiO_2/reduced graphene oxide. Synth Met 270:116583. https://doi.org/10.1016/j.synthmet.2020.116583

Tugba Saka E, Tekintas K (2020) Light driven photodegradation of 4-nitrophenol with novel Co and Cu phthalocyanine in aqueous media. J Mol Struct 1215:128189. https://doi.org/10.1016/j.molstruc.2020.128189

Wang J, Sui Q, Lyu S, et al (2020) Source apportionment of phenolic compounds based on a simultaneous monitoring of surface water and emission sources: A case study in a typical region adjacent to Taihu Lake watershed. Sci Total Environ 722:137946. https://doi.org/10.1016/j.scitotenv.2020.137946

Wang N, Lv G, He L, Sun X (2021a) New insight into photodegradation mechanisms, kinetics and health effects of p-nitrophenol by ozonation in polluted water. J Hazard Mater 403:123805. https://doi.org/10.1016/j.jhazmat.2020.123805

Wang Q, Wang P, Xu P, et al (2021b) Submerged membrane photocatalytic reactor for advanced treatment of p-nitrophenol wastewater through visible-light-driven photo-Fenton reactions. Sep Purif Technol 256:117783. https://doi.org/10.1016/j.seppur.2020.117783

Xiong Z, Lai B, Yang P (2018) Enhancing the efficiency of zero valent iron by electrolysis: Performance and reaction mechanism. Chemosphere 194:189–199. https://doi.org/10.1016/j.chemosphere.2017.11.167

Xiong Z, Zhang H, Zhang W, et al (2019) Removal of nitrophenols and their derivatives by chemical redox: A review. Chem Eng J 359:13–31. https://doi.org/10.1016/j.cej.2018.11.111

Yassumoto L, Monezi NM, Takashima K (2009) Decolorization of some azo dyes by direct photolysis and H_2O_2/UV processes. Ciências Exatas e Tecnológicas 30:117–124

Zhang SX, Sun FX, Zhu GS (2017) Porous aromatic framework as an efficient adsorbent in removing phenol from water. Inorg Chem Commun 85:110–112. https://doi.org/10.1016/j.inoche.2017.08.009

Zhao D, Ding C, Wu C, Xu X (2012) Kinetics of Ultrasound-Enhanced Oxidation of p-Nitrophenol by Fenton's Reagent. Energy Procedia 16:146–152. https://doi.org/10.1016/j.egypro.2012.01.025

Zhao S, Ma H, Wang M, et al (2010) Study on the mechanism of photo-degradation of p-nitrophenol exposed to 254 nm UV light. J Hazard Mater 180:86–90. https://doi.org/10.1016/j.jhazmat.2010.03.076

Supplementary Files

This is a list of supplementary files associated with this preprint. Click to download.

- ESMDegradationandMineralizationofPNFusingAOPs.docx